Title

Using Synchrotron Radiation Microtomography to Investigate Multi-scale Three-dimensional Microelectronic Packages.

Journal

Journal of Visualized Experiments, 2016(110)

ISSN

1940-087X

Authors

Carlton, Holly D

Elmer, John W

Li, Yan

et al.

Publication Date

2016

DOI

10.3791/53683

Peer reviewed

LAWRENCE
LIVERMORE
NATIONAL
LABORATORY

LLNL-JRNL-670598

Using Synchrotron Radiation micro-Tomography to Investigate Multi-scale Three-dimensional Microelectronic Packages

H. D. Barth, J. W. Elmer, Y. Li, M. Pacheco, D. Parkinson, A. A. MacDowell

May 11, 2015

Journal of Visualized Experiments

Disclaimer

TITLE:
Using Synchrotron Radiation micro-Tomography to Investigate Multi-scale Three-dimensional Microelectronic Packages

AUTHORS:
Carlton, Holly D
Materials Engineering Division
Lawrence Livermore National Laboratory
Livermore, CA USA
carlton4@llnl.gov

Elmer, John W
Materials Engineering Division
Lawrence Livermore National Laboratory
Livermore, CA USA
elmer1@llnl.gov

Li, Yan
Assembly Test and Technology Development Failure Analysis Labs
Intel Corporation
Chandler, AZ USA
yan.a.li@intel.com

Pacheco, Mario
Assembly Test and Technology Development Failure Analysis Labs
Intel Corporation
Chandler, AZ USA
mario.pacheco@intel.com

Goyal, Deepak
Assembly Test and Technology Development Failure Analysis Labs
Intel Corporation
Chandler, AZ USA
deepak.goyal@intel.com

Parkinson, Dilworth Y
Advanced Light Source,
Lawrence Berkeley National Laboratory
Berkeley, CA USA
dyparkinson@lbl.gov

MacDowell, Alastair A
Advanced Light Source,
Lawrence Berkeley National Laboratory

Berkeley, CA USA
aamacdowell@lbl.gov

CORRESPONDING AUTHOR:
Holly D. Carlton

KEYWORDS:
Synchrotron radiation micro-tomography, x-ray imaging, computed tomography, non-destructive failure analysis, lead free solders, and three-dimensional microelectronic packages.

SHORT ABSTRACT:
For this study synchrotron radiation micro-tomography, a non-destructive three-dimensional imaging technique, is employed to investigate an entire microelectronic package with a cross-sectional area of 16 x 16 mm. Due to the synchrotron's high flux and brightness the sample was imaged in just 3 minutes with an 8.7 μm spatial resolution.

LONG ABSTRACT:
Synchrotron radiation micro-tomography (SRμT) is a non-destructive three-dimensional (3D) imaging technique that offers high flux for fast data acquisition times with high spatial resolution. In the electronics industry there is serious interest in performing failure analysis on 3D microelectronic packages, many which contain multiple levels of high-density interconnections. Often in tomography there is a trade-off between image resolution and the volume of a sample that can be imaged. This inverse relationship limits the usefulness of conventional computed tomography (CT) systems since a microelectronic package is often large in cross sectional area 100-3600 mm^2, but has important features on the micron scale. The micro-tomography beamline at the Advanced Light Source (ALS), in Berkeley, CA USA, has a setup which is adaptable and can be tailored to a sample's properties, i.e. density, thickness, etc., with a maximum allowable cross-section of 36 x 36 mm. This setup also has the option of being either monochromatic in the energy range ~7-43 keV or operating with maximum flux in white light mode using a polychromatic beam. Presented here are details of the experimental steps taken to image an entire 16 x 16 mm system within a package, in order to obtain 3D images of the system with a spatial resolution of 8.7 μm all within a scan time of less than three minutes. Also shown are results from packages scanned in different orientations and a sectioned package for higher resolution imaging. In contrast a conventional CT system would take hours to record data with potentially poorer resolution. Indeed, the ratio of field-of-view to throughput time is much higher when using the synchrotron radiation tomography setup. The description below of the experimental setup can be implemented and adapted for use with many other multi-materials.

INTRODUCTION:
In the microelectronics field, as in many other fields, non-destructive evaluation at the micrometer scale is necessary when characterizing samples. Specifically for the microelectronics industry there is interest in probing 3D microelectronics packages, containing multi-levels and multi-materials, and identifying failures in packages during thermal, electrical,

and mechanical stressing of components. Around the world synchrotron radiation facilities have designated tomography and diffraction beamlines that are used for failure analysis of microelectronic packages. Some examples of this are imaging void formation caused by electromigration [1-3], evaluating mechanisms for tin whisker growth [4,5], in situ observations of undercooling and anisotropic thermal expansion of tin and intermetallic compounds (IMCs)[6,7], in situ observation of solidification and IMC formation [8-10], anisotropic mechanical behavior and recrystallization of tin and lead free solders[10], voids in flip chip bumps, and in situ observations of Ag-nanoink sintering[11]. All of these studies have further advanced the understanding and development of components in the microelectronic industry. However, many of these studies have focused on small regions within the package. More information could be gleaned from testing and characterizing the full size package using high resolution SRμT in order to further their development.

The electronic packages being produced now contain multiple layers of interconnects. These packages and devices are growing more and more complex which calls for a 3D solution for non-destructive evaluation with regard to failure analysis, quality control, reliability risk assessment, and development. Certain defects require a technique that can detect features less than 5 μm in size, which include voids and cracks forming inside copper substrate vias, identifying non-contact open and nonwet solder pads in multilevel packaging [12], locating and quantifying voids in ball grid arrays (BGAs) and C4 solder joints. During the substrate assembly process these types of defects must be identified and monitored extensively to avoid unwanted failures.

Currently CT systems using laboratory-based sources, also known as tabletop, are able to provide as high as ~1 μm spatial resolution, and are being used to isolate failures in multilevel packages with promising results. However, tabletop CT systems have some limitations when compared to SRμT setups [13,14]. Tabletop systems are limited to only imaging a certain density range of materials since they usually only contain one or two x-ray source spectrums. Also through-put-time (TPT) remains long for conventional tabletop CT systems requiring several hours of data acquisition time per 1-2 mm^2 region of interest, which can limit its usefulness; for instance, analyzing failures in Through Silicon Vias (TSV), BGAs or C4 joints often require acquiring multiple Field of Views (FoV) or regions of interest at high resolution within the sample, resulting in total TPT of 8-12 hours, which is a show stopper for conventional tabletop CT systems when multiple samples have to be analyzed. Synchrotron radiation provides much higher flux and brightness than conventional x-ray sources, resulting in much faster data acquisition times for a given region of interest. Although SRμT does allow for more flexibility with respect to types of materials that can be imaged and sample volume, it does have limitations, which are specific to the synchrotron source and setup used, specifically maximum acceptable thickness and sample size. For the SRμT setup at the ALS the maximum cross-sectional area that can be imaged is <36 x 36 mm and the thickness is limited by the energy range and flux available and is material specific.

This study is used to demonstrate how SRμT can be utilized to image an entire multi-level system in package (SIP) with high resolution and low TPT (3-20 minutes) for use in inspecting 3D

semiconductor packages. More details on comparing tabletop CT's to Synchrotron Source CT's can be found in references [13,14].

Experimental Overview & Beamline 8.3.2 Description:
There are synchrotron facilities available for tomography experiments around the world; most of these facilities require submission of a proposal where the experimentalist describes the experiment, as well as its scientific impact. The experiments described here were all performed at the ALS at Lawrence Berkeley National Laboratory (LBNL) at beamline 8.3.2. For this beamline there are two energy mode options: 1) monochromatic in the energy range ~7-43 keV or 2) polychromatic "white" light where the entire available energy spectrum is used when scanning high density materials. During a typical scan at beamline 8.3.2 a sample is mounted on a rotational stage where x-rays penetrate the sample, then the attenuated x-rays are converted into visible light through a scintillator, magnified by a lens, and then projected onto a CCD for recording. This is done while the sample rotates from 0 to 180° producing a stack of images that is reconstructed to obtain a 3D view of the sample with micrometer resolution. The resulting tomographic dataset size ranges from ~3-20 Gb depending on the scan parameters. Figure 1 shows a schematic of the hutch where the sample is scanned.

The following protocol presented here describes the experimental setup, data acquisition, and processing steps required for imaging an entire microelectronic package, but the steps can be modified to image a variety of samples. The modifications depend on the sample size, density, geometries, and features of interest. Table 1 and 2 present the resolution and sample size combinations available at beamline 8.3.2 (ALS, LBNL, Berkeley, CA). For the microelectronic package investigated here the sample was imaged using a polychromatic ("white") beam, which was selected due to the thickness and high-density of the sample's components. The sample was mounted in the horizontal orientation on a chuck mount, this orientation allowed for the entire sample to fit within the height of the beam, which is parallel with a height of ~4 mm and width of ~40 mm, therefore only requiring one scan to capture the entire sample.

PROTOCOL:

Note: Protocol details described below were written specifically for work at beamline 8.3.2 at the ALS, Berkeley, CA. Adaptations may be required for work at other synchrotron facilities, which can be found around the world. Appropriate safety and radiation training is required for running experiments at these facilities and the guidelines for training can be found on each individual synchrotron facility's website. Any changes or updates to the tomography protocol (ALS, LBNL, Berkeley, CA) can be found on the beamline manual http://microct.lbl.gov/manual. Other examples of work performed at the tomography beamline at the ALS is presented in Reference[15]. Details on the tomography process can be found in Reference[16]. The beamline scientists are available to answer any questions and will facilitate the experimental setup.

1. Steps for performing tomography scans at beamline 8.3.2 (ALS, LBNL)

1.1. Prepare the sample for the scan by mounting it on a sample holder designed to fit in the beamline's rotational stage. For samples that do not have a custom mount, adhere the sample to a post or drill chuck with clay or wax.

Note: The sample scanned in this study was a microelectronic package that is 16 x 16 mm and only ~3 mm in height. In order to fit the entire package in the field of view the sample was mounted horizontally using clay provided at the beamline.

1.1.1. Align the sample to ensure that when it rotates through 180 degrees it stays within the field of view. Before loading the sample on the rotational stage inside the hutch there is an offline mock rotation stage that is used to align the sample. Visual inspection of the center of rotation is usually sufficient for the alignment.

1.1.2. Mount the sample attached to the sample holder inside the hutch. Once the sample has been mounted in the hutch, two orthogonal centering motors allow positioning of the sample with respect to the center of rotation.

Note: Sometimes sample preparation is needed ahead of experiment time in order to make sure the sample size is correct for the desired resolution. For example, some of the 16 x 16 mm microelectronic packages were sectioned into smaller pieces for further high resolution scanning. The sample size can be determined using Tables 1 & 2.

1.2. Select the magnification for the scan based on the sample size and feature size of interest. Beamline 8.3.2 has several lenses to choose from which produce images with a range of pixel sizes from 0.35 – 9 µm. Depending on the magnification, the sample must be of appropriate cross-sectional area, as the field of view decreases with increasing magnification.

1.2.1. Since the sample scanned here is 22.6 mm in the longest direction the 1x lens with the PCO.4000 was selected, as shown in Table 1 and 2, this combination gives the largest sample field of view. The resulting pixel size is 8.7 µm.

1.3. Set the x-ray energy or switch to a polychromatic beam using the Beamline Control Computer. The x-ray energy range at beamline 8.3.2 is continuous from 4-80 keV, but the multilayer monochromator mounted limits the energy range to ~7-43 keV, while the peak flux occurs at ~12 keV. To get the best quality image, base the energy selection on targeting a ~30% transmission, which can be measured on the Data Acquisition Computer. In general, %Transmission increases with increasing energy.

1.3.1. For the microelectronic package, "white" light mode was selected due to the thickness and material of the package.

Note: The beamline 8.3.2 manual has detailed steps for changing between "white" light and monochromatic mode.

1.3.2. When using “white” light mode, add 2-4 metal aluminum and copper filters in line with the x-ray beam in order to filter out the lower energy x-rays. For this sample, 2 copper sheets with a total thickness of ~1.2 mm were used.

1.3.3. Calculate transmission through the sample ahead of time by using: http://henke.lbl.gov/optical_constants/filter2.html or http://www.nist.gov/pml/data/xraycoef/ http://11bm.xray.aps.anl.gov/absorb/absorb.php. For example, inputting the chemical formula and estimated thickness for the sample will output a graph showing the percent transmission as a function of energy range.

1.4. Verify that the stage’s center of rotation is aligned with the camera’s center. To check that the sample is aligned rotate it through 180 degrees using software on the Beamline Control Computer and visually observe the change in sample location by viewing the radiographs on the computer. Control changes to alignment on the same computer. Image quality deteriorates when the sample’s alignment is off enough so that regions of the sample leave the field of view during the sample rotation.

1.5. Manually set sample to detector distance for scan. The camera is on a translational stage that can move horizontally which is used to change the sample to detector distance. When the distance increases the phase contrast contribution also increases. Phase effects are helpful to more easily image subtle cracks and edges, but also cause other “halo effect” artifacts that are often undesirable.

1.6. Verify the beamline alignment. Check the focus of the image and adjust the focus motor if necessary. Confirm that the pixel size calibration is correct by moving the sample a defined amount and measuring the number of pixels the sample moved to calculate µm/pixel. The voxel size will change depending on the experimental setup.

1.6.1. Check that as the image moves horizontally, image features track horizontally along a constant pixel, and if not, adjust the camera tilt motor so that they do. This aligns the axis of rotation so that it is parallel to pixel columns, which is the alignment assumed later by the reconstruction algorithms.

1.7. Select an exposure time for each radiograph. The range for exposure time is 1 -1500 ms and the selection depends on the scan energy and resolution (which determines the observed flux per resolution element). The selected time should provide a tradeoff between the quickest scan time and a scan with more counts and thus the best signal-to-noise ratio.

1.7.1. For the microelectronic package, a scan time of 100 ms per exposure was selected.

Note: Make sure there are no saturated pixels or at least less than the recommended target of 100. The control system is set to display camera counts on a converted scale so that each camera’s maximum counts is 65,535.

1.8. Set up the Scan Parameters using the Data Acquisition Computer.

1.8.1. Input the desired angular range, and the number of images to collect over that range. The more angles selected the longer the scan times and larger the dataset size. Common numbers of angles are 513, 1025, and 2049 over a 0-180 degree range. For this study, use 1025 angles over 180 degrees during data acquisition.

1.8.2. Select the scanning mode. The two options for scanning mode are 1) normal and 2) continuous tomography. The continuous mode is preferred since it results in the shortest scan time, ~3 minutes. In this mode, the rotation stage continuously moves as images are collected. In normal mode, the rotation stage stops at each angle and then an image is collected.

1.8.3. Specify number of bright and dark field images. The bright and dark field images are necessary for performing reconstruction. For the dark field images the shutters close and for the bright field or background images the samples moves out of the field of view. Verify that the sample is translated far enough so that it is not present in the bright field image in order to avoid large defects in the reconstructed images. Here, acquire 15 dark field images and 15 bright field images.

1.8.4. Determine if tiling is necessary. If the sample is taller than the field of view there is a tiling option, which will scan the sample then translate it vertically until the entire sample is captured.

1.9. Execute run scan on the Data Acquisition Computer. The scan will run automatically based on the inputted settings.

2. Steps for performing Tomographic Data Processing.

2.1. Transfer data to an analysis computer available at the beamline to perform the reconstruction and filtering of the data set using beamline protocol. Reconstruction can run independent of the data acquisition.

Note: Data is automatically transferred to NERSC, a high performance computer, where it is processed and reconstructed. Users can sign up for an account at NERSC to access their data through the SPOT Suite web portal at spot.nersc.gov. This portal is still in development mode, so many users prefer to have more control over the reconstruction parameters, in which case they follow the remaining steps.

2.2. Reconstruct the raw images following these steps: 1) normalize images, 2) create stack of sinograms, 3) apply ring removal/filters, and 4) perform parallel beam reconstruction. The reconstruction is based on a filtered back projection algorithm. The reconstruction process results in TIFF images that contain information on the location and intensity of each pixel making up the sample volume. A schematic of the entire process is shown in Figure 2.

2.2.1. To access the plugin start FIJI (which is an acronym for Fiji Is Just ImageJ) and select the menu Plugins → ALSmicroCT → NormalizeStack832newnaming as shown below. A user at the ALS facility can perform the entire reconstruction process using a custom plugin for ImageJ/Fiji, which integrates several software packages designed to streamline the reconstruction process.

Note: Fiji and the plugin are available for use on multiple Beamline 8.3.2 analysis computers.

2.2.2. Once the FIJI dialog box is open, as shown below, select the raw file intended for reconstruction. The stack of raw, bright, and dark images should now be loaded.

2.2.3. Find the center of rotation by clicking 'Detect center of rotation', then to visualize the reconstructed image select 'Preview reconstruction'. The value for center of rotation can also be inputted manually and previewed.

2.2.4. Using this interface there is the option to change the ring removal parameters, the type of image (8, 16, or 32 bit), pixel range, rotation angle of images, and define cropped region. Each new parameter set can be visualized using the 'Preview reconstruction' button.

2.2.5. Once the parameters are selected, reconstruct the entire stack of images by selecting 'run'. All the subsequent data files can be found in the specified 'Output directory', the default directory will be in an output file within the raw data folder.

2.3. Access raw data from tomography scans from any computer by going to the website http://spot.nersc.gov/, which is the NERSC (LBNL supercomputer) server through the SPOT portal.

Note: Each individual researcher must have their own NERSC account to access their specific datasets. A user can setup an account at https://nim.nersc.gov/nersc_account_request.php. At the beamline, each research group is assigned a beamline account. This account is used to access beamline computers, and can also be used to access data directly from the beamline server using Globus Online.

2.4. Visualize the data in both 3D and 2D by loading the stack of 2D reconstructed images into any 3D analysis software. The samples and images presented here use Avizo software to perform the analysis and visualization, which is available to beamline users at any of the beamline 8.3.2 analysis computers.

2.5. After a data set is uploaded into the visualization software perform further data analysis to get quantified information on specific features within the sample. Often datasets are downsampled in order to reduce the output data size. However this can increase the voxel size reducing fidelity, but smooth the image view for easier segmentation.

2.5.1. Select segment features of interest by thresholding the histogram of the stack of 2D reconstructed slices and assigning a new pixel value to pixels that fall within a specified range.

2.5.2. Visualize segmented volumes and surfaces. Once features are segmented they are viewed in 3D using Avizo or any preferred visualization software. This allows for 3D surface renderings of specific features, like solder balls at a certain region of interest.

2.5.3. Quantify features in sample, i.e., crack size, vias, porosity, defects, etc. Once a feature of interest is identified, such as a via or crack, the feature can be segmented and volumetric information on crack width, length, via volume, porosity distribution can be quantified by evaluating the tomographic data set.

2.5.4. Create a movie of the sample showing the sample in different orientations. Movie 1 shows examples of the different cross-sectional views and volume rendering views for the microelectronic package imaged in the horizontal orientation.

REPRESENTATIVE RESULTS:

The images captured using tomography occur due to the differential absorption of x-rays in the solder interconnects, metallic traces, and other materials in the microelectronic package as a function of the different attenuation lengths and thickness of these multi-materials. The SIP package consisted of a silicon die attached to a ceramic substrate with first level interconnect (FLI) flip chip C4 solder balls of approximately 80 µm diameter; mid-level interconnect (MLI) solder balls of approximately 350 µm connecting this substrate to an FR4 epoxy circuit board; and second level interconnect (SLI) BGA solder balls of approximately 650 µm on the back side of the circuit board. Figure 2 shows a schematic of the sample when it is placed in the horizontal orientation; this orientation was selected in order to fit the entire sample in the field of view for one scan. Figure 3 shows the 3D images from the same sample, an entire package, which was imaged in one scan with low TPT (Table 2). This data was analyzed and prepared using Avizo. For the microelectronic packages an angular increment of 0.175° was selected resulting in 1025 images over 180 degrees. In Figure 3a the plate through holes, copper vias, and some of the substrate are visible. Figure 3b zooms in on a region of interest showing one corner of the field programmable gate array (FPGA) die and substrate. This shows how quickly the individual components of an entire multilevel package can be inspected. Figure 4 demonstrates the features detected with SRµT in a FPGA SIP package. Here the circuit board, VIA's, silicon die, both substrates, and all levels of interconnects are discernible. Figure 5 and 6 demonstrate the use of tomography data to visualize features in 3D, where two different views of the interconnects are displayed. Figure 6 shows a 3D image of the vertically scanned CPU die package with FLI and MLI connections. Due to the vertical scan orientation the entire samples was not captured in one scan, in order to image the entire sample in this orientation tiling would be necessary. Figure 6b shows a 2D tomographic slice magnified; here the image quality is sufficient to observe pores within a solder ball, which were created during extended thermal cycling prior to imaging.

Figure 1. Schematic showing tomography setup. Schematic of the hutch at beamline 8.3.2 at the Advanced Light Source (Lawrence Berkeley National Laboratory, Berkeley CA USA). (Figure taken from 8.3.2 Microtomography Manual, and can be accessed at:

http://microct.lbl.gov/manual)

Figure 2. Steps for reconstructing data. Schematic showing the steps to get a final 3D reconstructed image of a sample from the tomography setup. The sample here is a 16 x 16 mm SIP package being imaged in the horizontal orientation.

Figure 3. 3D volume rendering of package. 3D rendering of an entire FPGA SIP package imaged with 8.7 um resolution and a scan time of 3 minutes (a) shows the entire package, and (b) zoomed-in view of a region of the package showing one corner of the FPGA substrate and the circuit board interconnections.[13]

Figure 4. Tomographic image showing a cross-section of the package. 2D reconstructed slice taken through the FPGA SIP package. This sample was imaged with 4.5 µm resolution and a scan time of 20 minutes. The silicon die, underfill, both substrates, and all levels of interconnects can be observed.[13]

Figure 5. 3D volume rendering of the three interconnect levels. Segmented 3D image showing the entire SIP package with an 8.7 µm resolution (3 min. scan time). This shows the three levels of interconnects (FLI, MLI, and SLI).[13]

Figure 6. Visible pores identified in a solder ball. (a) 3D reconstructed image of the vertically scanned CPU die package with FLI and MLI solder connections. (b) Zoomed in region of a 2D reconstructed slice, showing a MLI solder ball with a large center void and cracks caused during intentional thermal stress testing.[13]

Movie 1. Tomography images in 3D and 2D of the package. This movie shows the 3D volume rendering of the 16 x 16 mm^2 package from different perspectives. Then pans through the different slices to show internal information from within the package.

Table 1. Details showing the cameras and lenses available at ALS beamline 8.3.2.

Table 2. Summary of resolutions, field of view, and imaging time for different cameras and lens options.

DISCUSSION:

All of the steps described in the protocol section are critical to obtaining high-resolution images of multi-scale and multi-material samples. One of the most critical steps is the sample mounting and the focusing of optics, which are vital to obtaining quality images that can be used for quantification. Specifically, even slight movement of the sample would cause artifacts in the reconstructed image and defocusing would cause deterioration in resolution. To avoid issues with image quality it is important to reconstruct a test image, which can take place simultaneously while the next sample scans. This will help identify any issues or problems that may have occurred during the scan setup. If there are problems with the reconstructed image it might be necessary to re-scan the sample paying careful attention to sample mounting and

alignment. During setup other issues may arise, such as errors with Labview, problems with the sample stage motor, or the absence of the x-ray beam. There are detailed steps for troubleshooting on the beamline's manual, which can be found on beamline website. Consult the beamline scientists to discuss further options for improving image quality or if the experimentalist comes across a problem not covered in the manual.

All of the figures shown here highlight the benefits of using SRμT to image an entire multi-level microelectronic package in only a few minutes with high spatial resolution and the ability to perform analysis on specific features within the sample non-destructively. For the samples imaged here the reconstruction time took under an hour. The wide energy spectrum at the ALS enables imaging of both high and low atomic number elements with the appropriate filtering. This allows for quantification of cracks, voids, delamination, defects, and much more. For several of the samples imaged here the continuous tomography mode aided in the fast data acquisition times. Although there is a wide range of materials and volumes that can be imaged using SRμT there are several limitations due to the available energy range for the ALS synchrotron facility. Specifically, the thickness of highly dense materials can be constrained.

This high-resolution capability of the synchrotron source CT system provides valuable information for both failure analysis and assembly process development. In contrast the tabletop CT system's relatively low brightness cannot allow for selection of a monochromatic energy and has difficulty highlighting defects in the presence of copper or solder surrounding features. The ability of a tomography technique to accommodate large sample sizes with faster TPT time is of the upmost importance to the semiconductor industry. The results obtained using SRμT suggest a path forward for new applications in microelectronics[14]. Overall there's a wide range of possibilities in this field for future work, specifically investigating these multi-material multi-scale microelectronic packages under in situ conditions, such as cycling temperature and cyclic loading.

ACKNOWLEDGMENTS:
The LLNL portion of this work was performed under the auspices of the U.S. Department of Energy by Lawrence Livermore National Laboratory under Contract DE-AC52-07NA27344. The Intel Corporation authors would like to thank Pilin Liu, Liang Hu, William Hammond, and Carlos Orduno from Intel Corporation for some of the data collection and helpful discussions. The Advanced Light Source is supported by the Director, Office of Science, Office of Basic Energy Sciences, of the U.S. Department of Energy under Contract No. DE-AC02-05CH11231.

DISCLOSURES:
The authors have nothing to disclose.

REFERENCES

1 Tian, T. *et al.* Quantitative X-ray microtomography study of 3-D void growth induced by electromigration in eutectic SnPb flip-chip solder joints. *Scr. Mater.* **65**, 646-649, doi:10.1016/j.scriptamat.2011.07.002 (2011).

2 Tian, T. *et al.* Rapid diagnosis of electromigration induced failure time of Pb-free flip chip solder joints by high resolution synchrotron radiation laminography. *Appl. Phys. Lett.* **99**, 082114, doi:10.1063/1.3628342 (2011).
3 Lee, A., Liu, W., Ho, C. E. & Subramanian, K. N. Synchrotron x-ray microscopy studies on electromigration of a two-phase material. *J. Appl. Phys.* **102**, 053507,doi:10.1063/1.2777122 (2007).
4 Sarobol, P. *et al.* Effects of local grain misorientation and β-Sn elastic anisotropy on whisker and hillock formation. *J. Mater. Res.* **28**, 747-756, doi:10.1557/jmr.2012.430 (2013).
5 Sarobol, P. *et al.* Recrystallization as a nucleation mechanism for whiskers and hillocks on thermally cycled Sn-alloy solder films. *Mater. Lett.* **99**, 76-80, doi:10.1016/j.matlet.2013.02.066 (2013).
6 Elmer, J. & Specht, E. Measurement of Sn and In Solidification Undercooling and Lattice Expansion Using In Situ X-Ray Diffraction. *J. Electron. Mater.* **40**, 201-212, doi:10.1007/s11664-010-1438-3 (2011).
7 Elmer, J., Specht, E. & Kumar, M. Microstructure and In Situ Observations of Undercooling for Nucleation of β-Sn Relevant to Lead-Free Solder Alloys. *J. Electron. Mater.* **39**, 273-282, doi:10.1007/s11664-010-1080-0 (2010).
8 Gourlay, C. M. *et al.* In situ investigation of unidirectional solidification in Sn–0.7Cu and Sn–0.7Cu–0.06Ni. *Acta Mater.* **59**, 4043-4054, doi:10.1016/j.actamat.2011.03.028 (2011).
9 Ma, H. T. *et al.* In-situ study on growth behavior of Ag3Sn in Sn–3.5Ag/Cu soldering reaction by synchrotron radiation real-time imaging technology. *J. Alloys Compd.* **537**, 286-290, doi:10.1016/j.jallcom.2012.05.055 (2012).
10 Zhou, B. *et al.* In Situ Synchrotron Characterization of Melting, Dissolution, and Resolidification in Lead-Free Solders. *J. Electron. Mater.* **41**, 262-272, doi:10.1007/s11664-011-1785-8 (2012).
11 Elmer, J. & Specht, E. D. In-Situ X-Ray Diffraction Observations of Low-Temperature Ag-Nanoink Sintering and High-Temperature Eutectic Reaction with Copper. *Metall. Mater. Trans. A* **43**, 1528-1537, doi:10.1007/s11661-011-0717-9 (2012).
12 Li, Y., Moore, J. S., Pathangey, B., Dias, R. C. & Goyal, D. Lead-Free Solder Joint Void Evolution During Multiple Subsequent High-Temperature Reflows. *IEEE Trans. Device Mater. Rel.* **12**, 494-500, doi:10.1109/TDMR.2012.2190736 (2012).
13 Elmer, J. *et al.* Synchrotron Radiation Microtomography for Large Area 3D Imaging of Multilevel Microelectronic Packages. *J. Electron. Mater.* **43**, 4421-4427, doi:10.1007/s11664-014-3375-z (2014).
14 Yan Li *et al.* High Resolution and Fast Throughput-time X-ray Computed Tomography for Semiconductor Packaging Applications,. *in Proceedings of the 64th IEEE Electronic Components and Technology Conference (ECTC).* 1457-1463 (2014).
15 McElrone, A. J., Choat, B., Parkinson, D. Y., MacDowell, A. A. & Brodersen, C. R. Using High Resolution Computed Tomography to Visualize the Three Dimensional Structure and Function of Plant Vasculature. *J Vis Exp*, e50162, doi:10.3791/50162 (2013).

16 Kinney, J. H. & Nichols, M. C. X-Ray Tomographic Microscopy (XTM) Using Synchrotron Radiation. *Annu. Rev. Mater. Sci.* **22**, 121-152, doi:10.1146/annurev.ms.22.080192.001005 (1992).

Acronyms:

ALS - Advanced light source
CT - Computed Tomography
FGPA - Field Programmable Gate Array
FLI - First Level Interconnect
FOV - Field of View
PTHs - Plated-Through Holes
MLI - Mid Level Interconnects
ROI - Region of Interest
SRμT– Synchrotron radiation micro-tomography
SLI - Second Level Interconnect
SIP – System in Package
TPT - Through put time
LLNL - Lawrence Livermore National Laboratory
LBNL – Lawrence Berkeley National Laboratory
NERSC - National Energy Research Scientific Computing Center

Figures

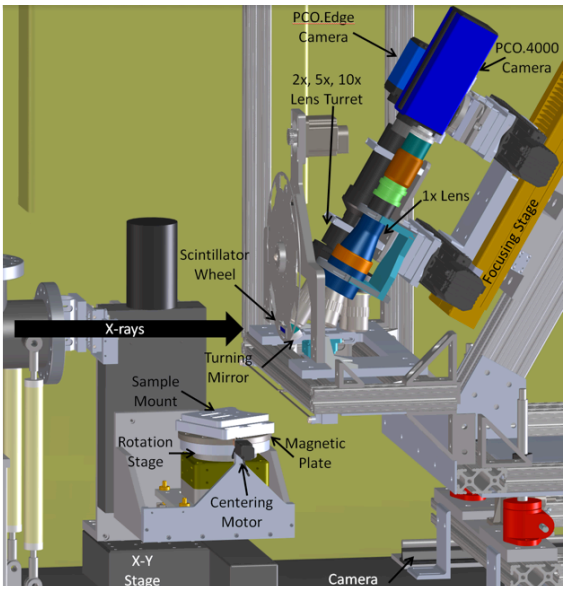

Figure 1. Schematic of the hutch at beamline 8.3.2 at the advanced light source (Lawrence Berkeley National Laboratory, Berkeley CA USA). (Figure taken from 8.3.2 Microtomography Manual, and can be accessed at: http://microct.lbl.gov/manual)

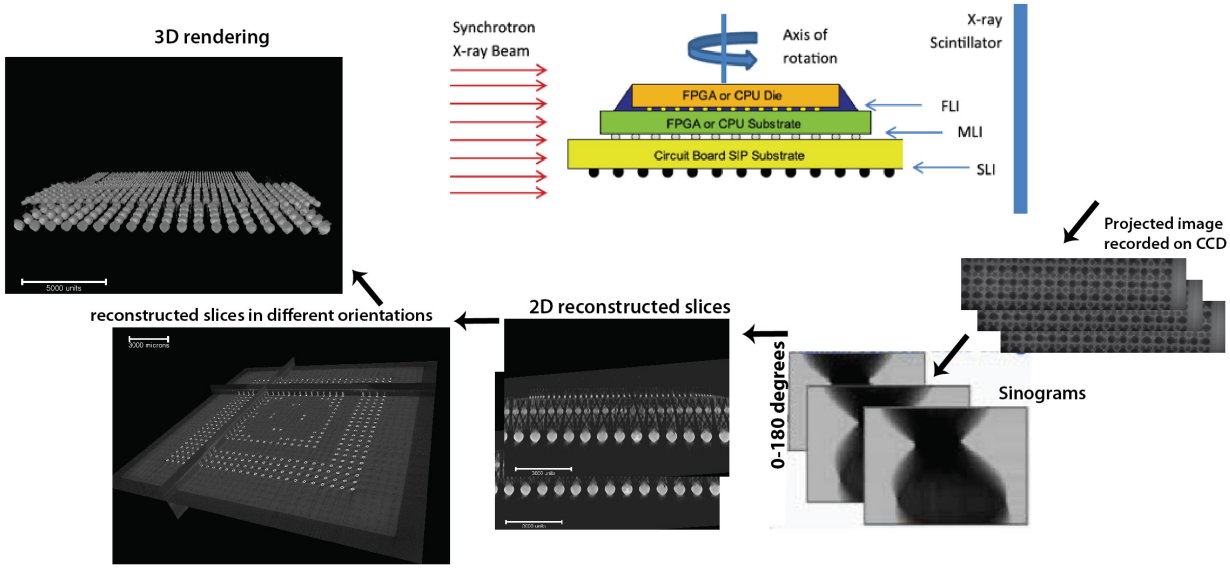

Figure 2: Schematic showing the steps to get a final 3D reconstructed image of your sample from the tomography setup. The sample here is a 16 x 16 mm^2 SIP package being imaged in the horizontal orientation.

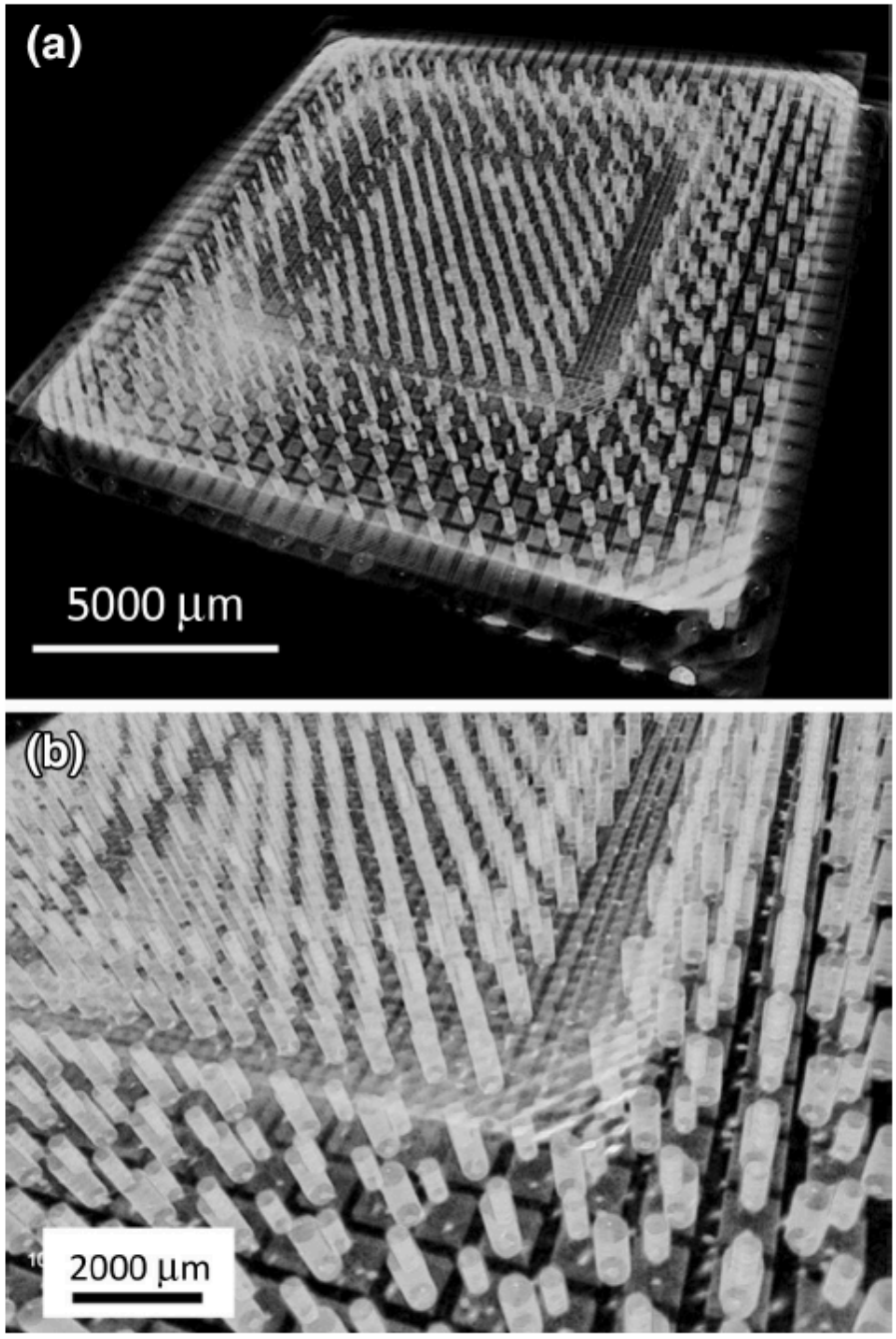

Figure 3. 3D rendering of an entire FPGA SIP package imaged with 8.7 um resolution and a scan time of 3 minutes (a) shows the entire package, and (b) zoomed-in view of a region of the package showing one corner of the FPGA substrate and the circuit board interconnections. (Ref. 13).

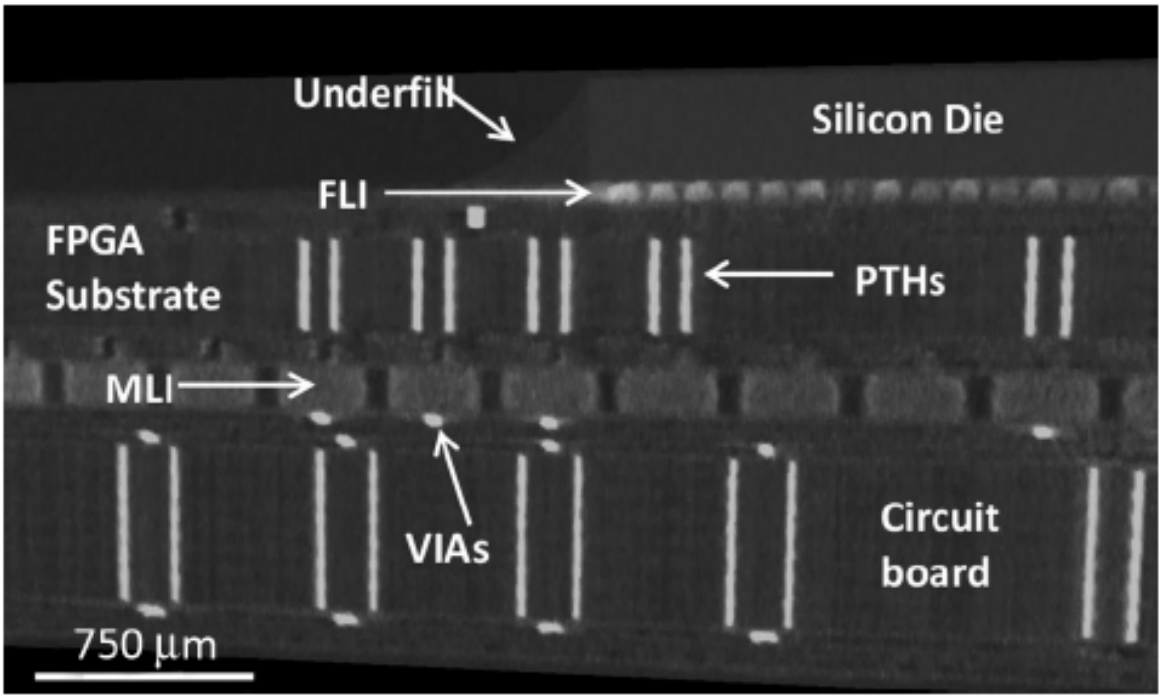

Figure 4. 2D reconstructed slice taken through the FPGA SIP package. This sample was imaged with 4.5 um resolution and a scan time of 20 minutes. The silicon die, underfill, both substrates, and all levels of interconnects can be observed. (Ref. 13).

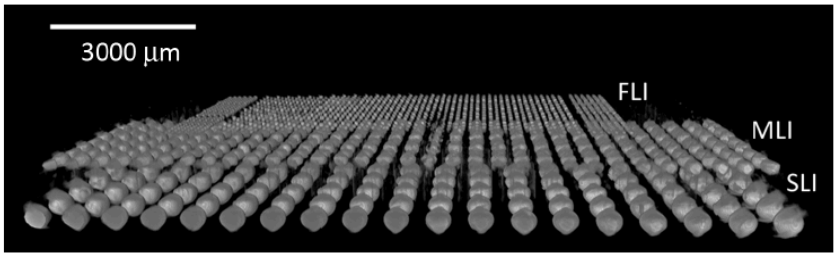

Figure 5. Segmented 3D image showing the entire SIP package with a 8.7 um resolution (3 min. scan time). This shows the three levels of interconnects (FLI, MLI, and SLI). (Ref. 13)

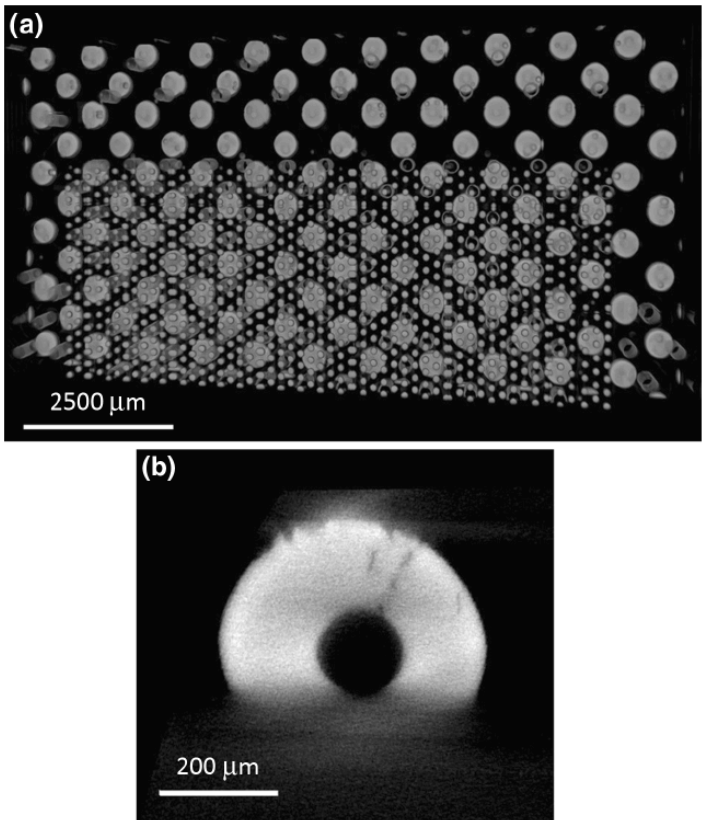

Figure 6. (a) 3D reconstructed image of the vertically scanned CPU die package with FLI and MLI solder connections. (b) Zoomed in region of a 2D reconstructed slice, showing a MLI solder ball with a large center void and cracks caused during intentional thermal stress testing. (Ref. 13)

Table 1. Details regarding available cameras and lenses at ALS beamline 8.3.2.

	PCO.4000 (4008x2672)		**PCO.Edge (2560x2160) [Optique Peter]**	
Lens	**Pixel (µm)**	**Field of view (mm)**	**Pixel (µm)**	**Field of view (mm)**
20x	--	--	-[0.33]	-[0.8]
10x	0.9	3.6	0.65 [0.69]	1.7 [1.7]
5x	1.8	7.2	1.3 [1.72]	3.3 [4.4]
2x	4.5	18	3.25 [3.44]	8.3 [8.8]
1x	9	36	6.5 [-]	16.6 [-]

Table 2. Summary of resolutions, field of view, and imaging time for different cameras and lens options.

Source	Resolution option	Camera/lens mag.	Pixel size (μm)	FOV width (mm)	FOV height (mm)	Image time TPT (min)	FOV/TPT (mm^2/min)
Synchrotron	Low	A/1×	8.7	36.0	6	3	72.0
ALS BL 8.3.2	Low	B/1×	6.5	16.6	6	3	33.2
	Med	B/2×	3.3	8.3	6	3	16.6
	Med	A/2×	4.5	18.0	6	20	5.4
	High	B/5×	1.3	3.3	2.8	5	1.84
	High	B/10×	0.65	1.7	1.4	11	0.22
Laboratory-based source (10 W; 40–60 kV)	High	–	1.5–2	1.5–2	1.5–2	180–240	~0.02

The scan time is indicated as *TPT* as a point of reference.